Approved for Public Release

Bubble Plumes and Breaking Waves: Measurements from R/P *FLIP*, January 1992

by Peter H. Dahl and Andrew T. Jessup

Technical Memorandum
APL-UW TM2-92
May 1992

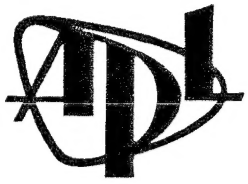

Applied Physics Laboratory University of Washington
1013 NE 40th Street Seattle, Washington 98105-6698

Contract N00039-91-C-0072

ACKNOWLEDGMENTS

We extend our thanks to the following people who made special contributions to this experiment: Jim Osse, Ron Stein, and Tim Wen from APL-UW; the R/P FLIP *crew led by Dewitt Efird; Fred Fisher of MPL, who contributed many ideas in the planning stages and made key logistical arrangements; Eric Slater of SIO, who gave valuable advice; Serhad Atatürk and Ralph Monis from the UW Department of Atmospheric Sciences; and Bill Keller of NRL and Ken Melville of SIO, who loaned the scatterometers. This work was supported by the Office of Naval Research, Code 124.*

ABSTRACT

This report is the first in a series of three covering APL-UW measurements of bubble plumes and breaking waves from R/P *FLIP* off the coast of California in January 1992. The overall objective of the experiment was to obtain realistic parameterizations of bubble plumes for use in models that predict low-frequency surface reveberation. The principal measurement objective was achieved: simultaneous, *in situ* measurements of bubble plumes and breaking waves using acoustic, microwave, and video systems trained on the same surface patch of the ocean. This report briefly summarizes the experiment, the range of environmental conditions encountered, the method of aligning the instruments, and the type and quantity of data gathered. Examples of acoustic data are given which clearly show bubble field growth; the appearance of one of these plumes was coincident with a wave-breaking event that was simultaneously detected with the microwave and video systems.

CONTENTS

LIST OF FIGURES

1. INTRODUCTION

Models that predict low-frequency surface reverberation require realistic parameters describing the bubble field. However, little is known about the space and time scales of the large, transient bubble plumes that originate from breaking waves, which may be critical inputs to acoustic reverberation models. The objective of this work, sponsored by ONR Code 124, was to obtain realistic parameterizations of bubble plumes derived from *in situ* ocean measurements. Our measurement goals were to (1) isolate individual wave-breaking events on the sea surface, (2) measure the bubble plumes generated by the breaking wave, and (3) relate our measurements to sea state conditions. To do this we made vertical-incidence acoustic measurements sensitive to subsurface bubbles simultaneously with oblique-incidence microwave measurements capable of detecting individual breaking waves and providing a measure of the overall degree of wave breaking. The measurement area on the sea surface was also videotaped, with the acoustic, microwave, and video data synchronized in time.

The measurements reported here were carried out in conjunction with a separate experimental effort in which APL-UW measured acoustic surface reverberation from the research platform *FLIP*, and the Institute of Ocean Sciences (IOS) measured the bubble field using its SEASAT instrument package deployed from USNS *De Steiguer* (T-AGOR-12), which kept station nearby. APL-UW received funding for that work from ONT; ARL/PSU provided technical management. The participation of IOS was under the auspices of The Technical Cooperation Program (TTCP). An overview of the *FLIP-De Steiguer* measurement series is given in Appendix A.

This report is the first in a series of three covering the measurements of bubble plumes and breaking waves from *FLIP*. Here we summarize the experiment, the range of environmental conditions encountered, the method of aligning our acoustic, microwave, and video instrumentation, and the type and quantity of bubble plume data gathered. We also present examples of acoustic data processed into images that clearly show bubble field growth. The appearance of one of these plumes was coincident with a wave-breaking event that was simultaneously detected from above with microwave and video systems.

2. FLIP CRUISE SCHEDULE

3–10 Jan 92	APL-UW loadout on *FLIP*
10 Jan	USNS *De Steiguer* departs San Diego en route to experiment site (34° N, 123° W)
11 Jan	*FLIP* departs San Diego in tow from the Navy tug *Navajo*; a test flip is completed outside San Diego harbor
12 Jan	*De Steiguer* arrives at site
13 Jan	*FLIP* arrives at site
16 Jan	*FLIP-De Steiguer* measurements begin
18 Jan	Plume boom acoustic systems fully operational
24 Jan	*De Steiguer* departs station en route to San Diego
2 Feb	Last day of measurements from *FLIP*
3 Feb	*Navajo* arrives on station (31° N, 125° W) and begins towing *FLIP* to San Diego
5 Feb	*FLIP* arrives in San Diego; APL-UW begins offload

Figure 1 shows *FLIP*'s drift track during the experiment.

3. ENVIRONMENTAL MEASUREMENTS

The following environmental measurements were made from *FLIP*:

1. conductivity, temperature, pressure (CTD)
2. wind speed and direction
3. air temperature, sea temperature, relative humidity
4. surface displacement
5. horizontal current velocity.

A meteorological station consisting of a propeller vane anemometer, an aspirated air temperature probe, and a shielded relative humidity sensor was mounted on the port boom at a height of 10 m above the sea surface. A second anemometer was mounted in the crow's nest at a height of 25 m. Sea surface temperature was provided by a thermistor mounted on the hull at a depth of 5 m. Figures 2 and 3 are time series of 10-min averages summarizing these measurements. Wave height measurements were provided by a commercial wire wave gauge mounted on the port boom. Unfortunately, the instrument was plagued by an intermittent grounding problem

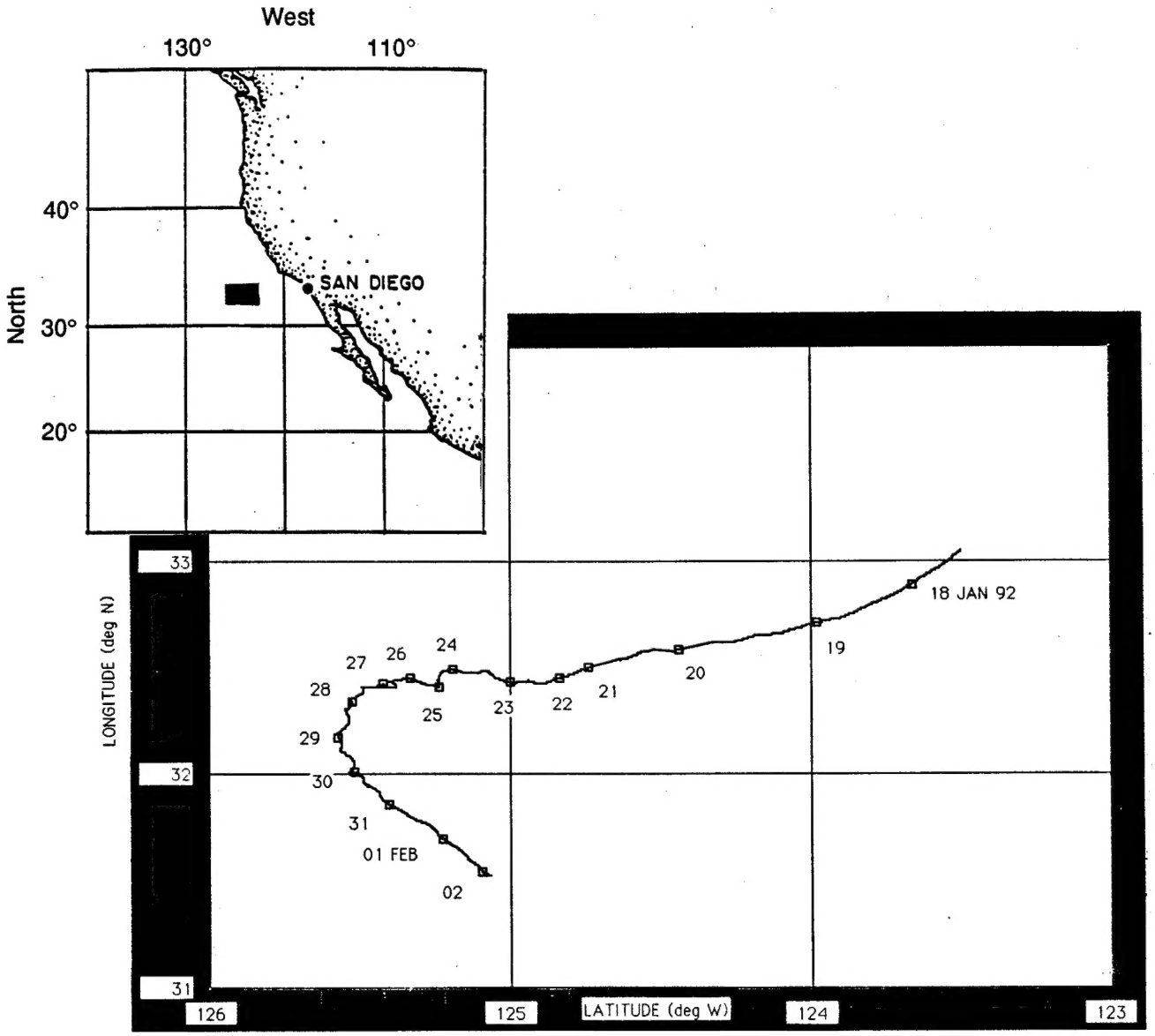

Figure 1. R/P *FLIP* drift track from GPS navigation system. Locations at 0000 hours local time are indicated along the track.

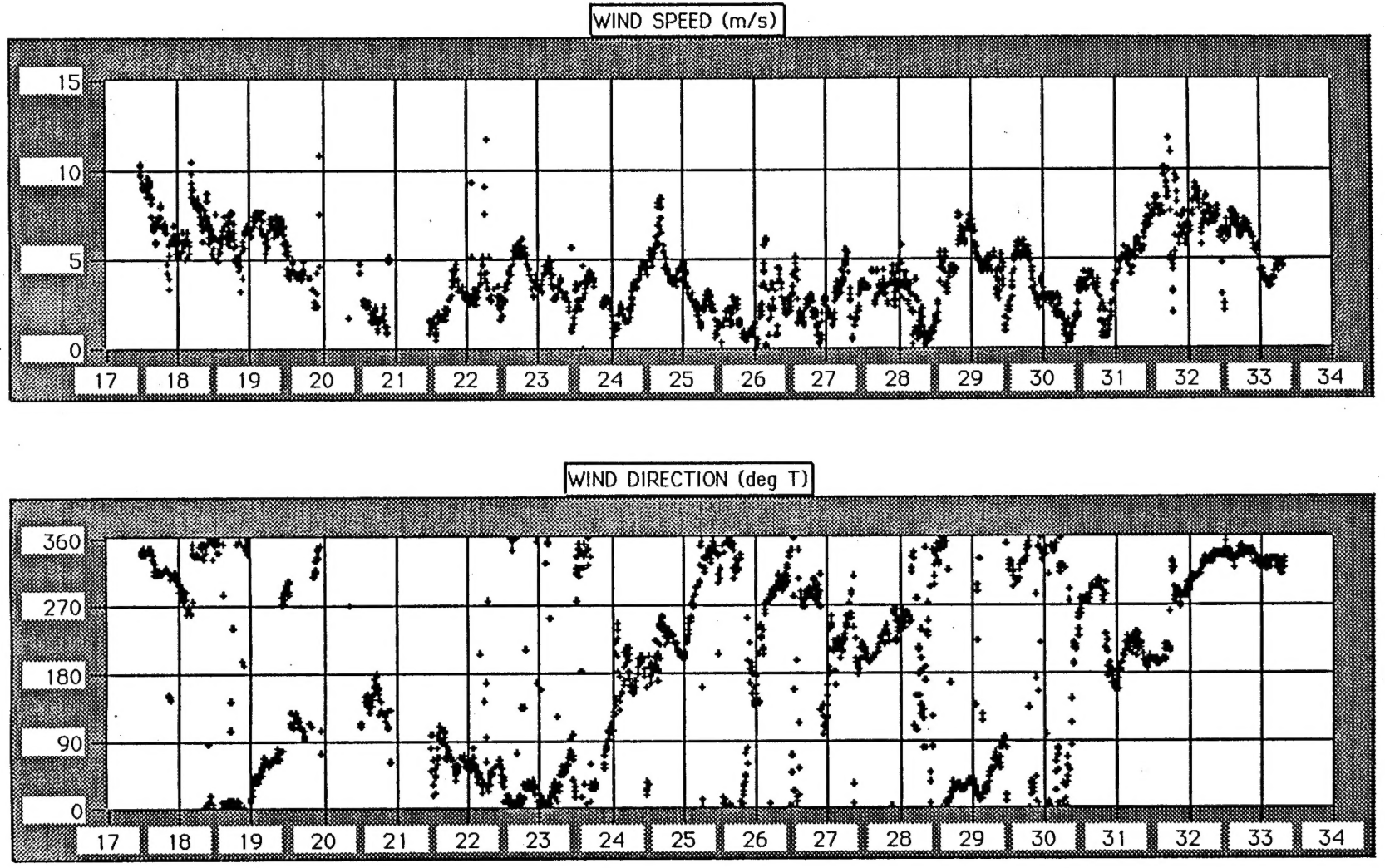

Figure 2. Time series of wind speed and direction for the duration of the experiment. The horizontal axis is in Year Days (1 Jan is Day 1). These data contain a few outliers due to interference from RF radio transmissions.

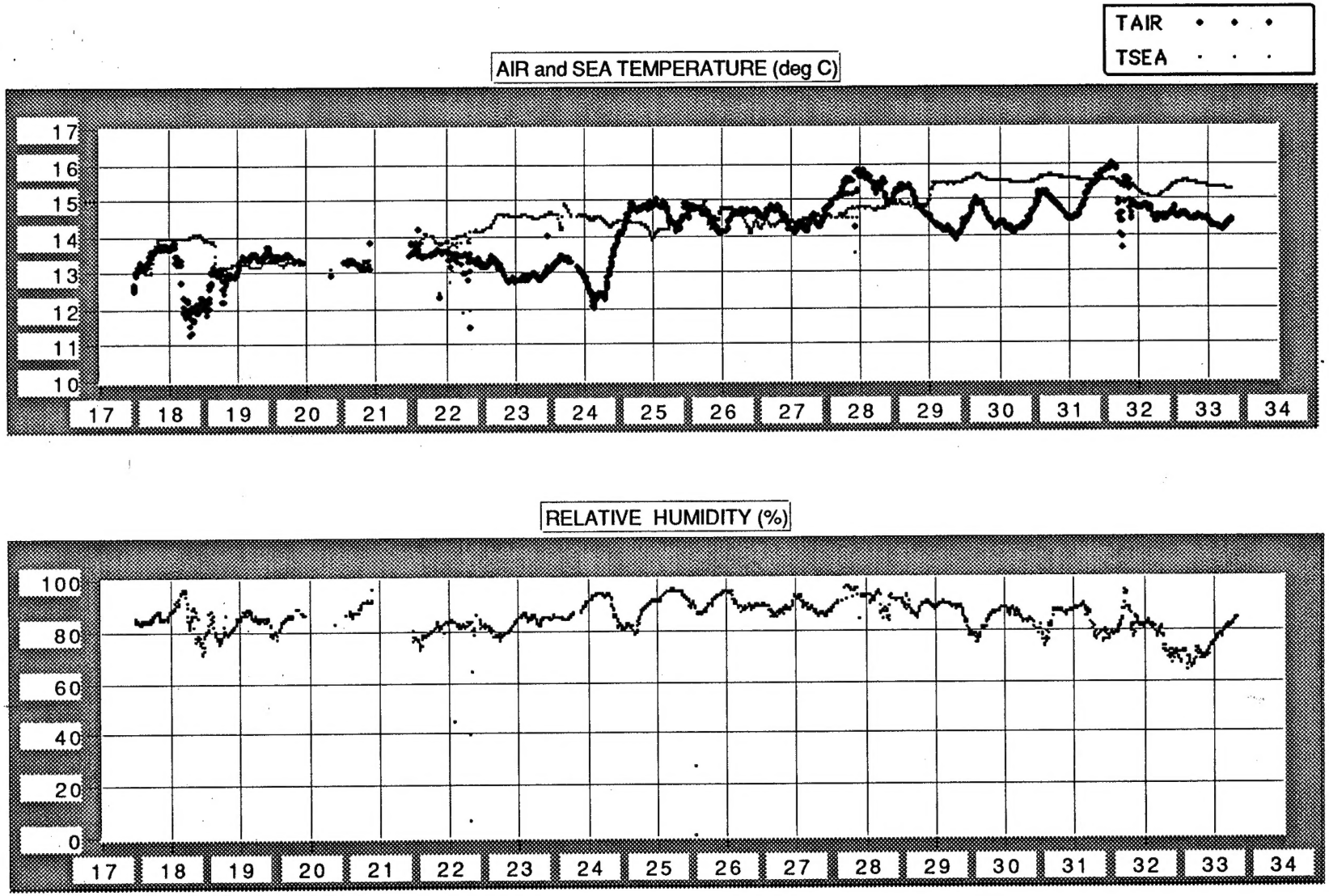

Figure 3. Time series of air temperature, sea temperature, and relative humidity for the duration of the experiment. The horizontal axis is in Year Days (1 Jan is Day 1). These data contain a few outliers due to interference from RF radio transmissions.

that significantly degraded the data. Because of this problem, the spare scatterometer was deployed at vertical incidence from the port boom to supplement the wave gauge. Figure 4 is an example of a surface displacement spectrum derived from the Doppler frequency output of the vertical-incidence scatterometer. The spectra contain useful data out to a frequency of roughly 1 Hz, above which the slope begins to flatten out. According to linear wave theory, a wave with frequency of 1 Hz has a wavelength of approximately 1.6 m. This cutoff is consistent with the finite size of the two-way, 3-dB illuminated area, which in this case was a circle of diameter 0.8 m. Other environmental instrumentation included an InterOcean S4 current meter, suspended from the port boom, and a Sea-Bird CTD used twice daily to make casts to 100 m.

4. SUBSURFACE PLUME BOOM ACOUSTIC SYSTEMS

Vertical-incidence acoustic measurements of bubble plumes were made from a 40-ft boom attached to *FLIP*'s hull 100 ft below the water line. The subsurface boom (Fig. 5), dubbed the "plume boom," was made of galvanized steel, trussed antenna mast sections. It extended upon flipping and was oriented approximately 45° off *FLIP*'s topside (aft) centerline. A 30-lb instrument package consisting of acoustic transducers and a pressure sensor was mounted on the tip of the boom.

We alternated between two acoustic systems to measure active sonar backscattering from bubbles. One was a Mk 46 torpedo head array with four subbeams; we collected data on four channels by transmitting on the sum beam and receiving on the individual subbeams. For the images reported here, we combined the four subbeam channels to produce a sum beam with, for example, a width of 20° at 30 kHz. Later we will cross-correlate the subbeam data to obtain more information on the structure of transient bubble clouds. We used the Mk 46 in two modes: multifrequency, in which we stepped between 20 and 50 kHz in 10-kHz steps every 250 ms, and single frequency, in which we used primarily 30 and 40 kHz. Our frequency range of 20–50 kHz spanned the equivalent resonant-scattering bubble radius of 160 to 64 μm.

The other acoustic system was a 2-inch circular piston transducer with a beam width of 8° from which we made single-channel measurements at 240 kHz, equivalent to a resonant-bubble radius of $\sim$ 13 μm. The two systems gave us good bubble size coverage (bracketing the nominal peak in the bubble size spectrum at $\sim$ 20 μm) and flexibility in beam-pattern-defined sampling volume.

For most of the measurements, we used a 0.5-ms pulse length (0.37-m vertical resolution); in a few cases, the pulse length was 1 ms. Data were gathered at either a 4-Hz ping rate for capturing transient bubble-plume features or a 1-Hz ping rate for obtaining background bubble-field data. Data were gathered in units ranging from 100 s to 10 min.

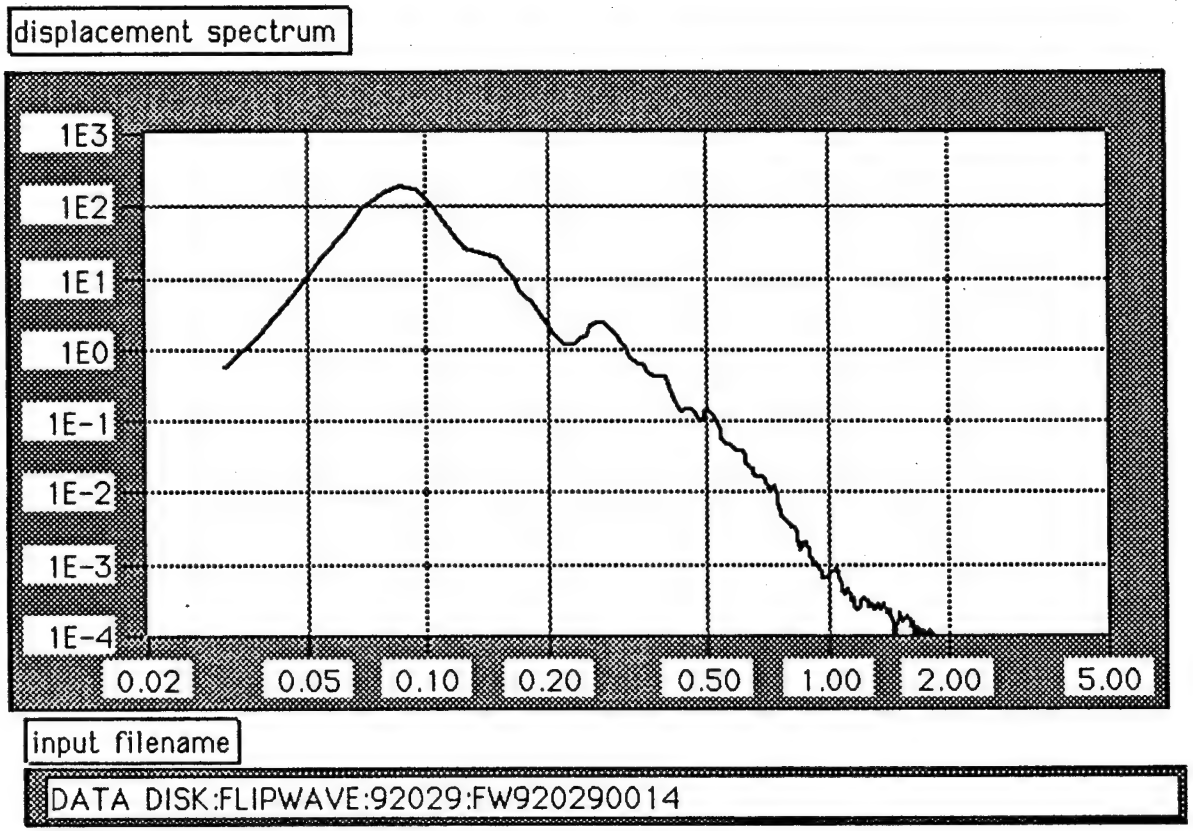

Figure 4. Example of surface displacement spectrum derived from Doppler-frequency output of vertical-incidence scatterometer. The vertical axis is logarithmic in arbitrary units. In this example, the sea conditions were dominated by large swell corresponding to the major frequency peak at 0.9 Hz. A wind-wave peak at 0.27 Hz is also evident.

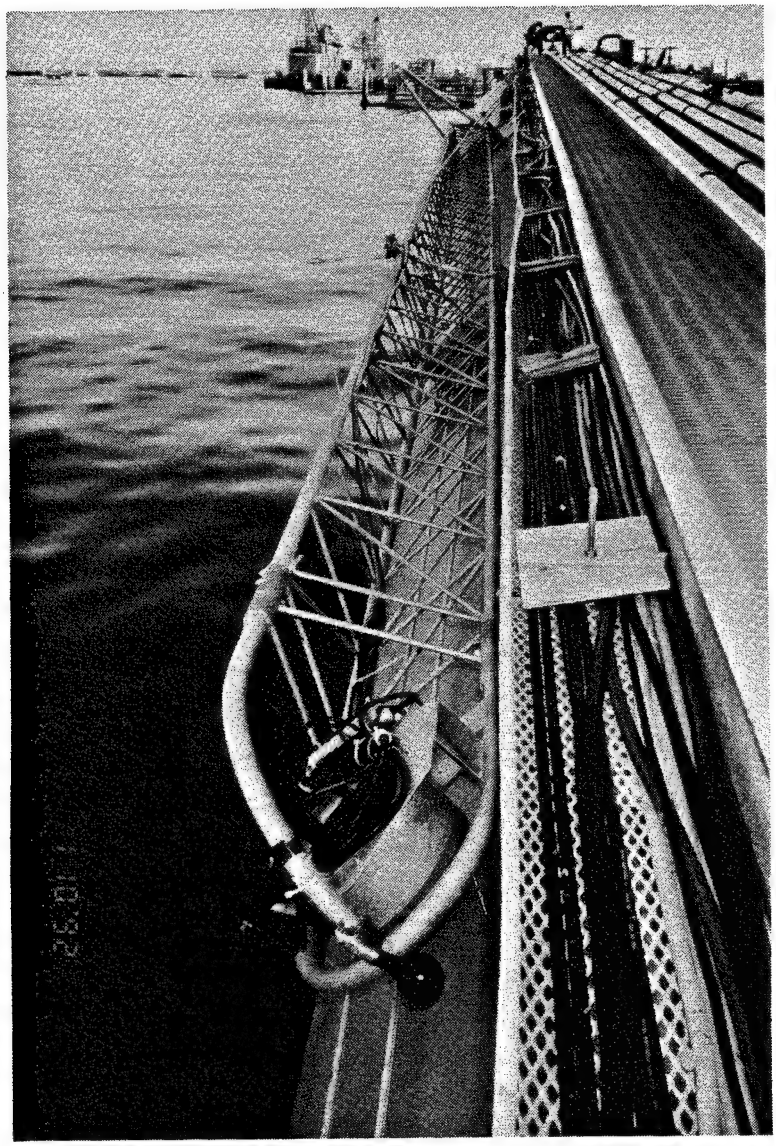

Figure 5. Photograph of the plume boom alongside *FLIP*'s hull; the instrument package can be seen at the tip of the boom.

For each ping, we recorded *FLIP*'s pitch, roll, heave, and direction. Pressure data from the sensor mounted on the instrument package were also recorded for each ping; these will serve as a measure of the instantaneous height of the water column above the transducers. This transducer-to-surface height is useful in sorting out the surface return from strong bubble-scatter returns.

5. AFT BOOM MICROWAVE AND VIDEO SYSTEMS

Continuous microwave and video measurements of breaking waves were made with a scatterometer and a video camera. Figure 6 shows the dual-polarized, Ku-band (14 GHz) Doppler scatterometer and video camera mounted on the aft boom at an incidence angle of 60^o approximately 8 m above the sea surface. In this configuration, the two-way, 3-dB illuminated area was an ellipse with dimensions 1.3 m $\times$ 2.6 m. The horizontal field of view of the video image was approximately 16 m. Preliminary processing of the microwave data consists of computation of radar cross section, mean Doppler frequency, and Doppler bandwidth. These quantities correspond to the backscattered power, the line-of-sight surface velocity, and the range of velocities within the illuminated area, respectively.

6. ALIGNMENT OF ACOUSTIC, MICROWAVE, AND VIDEO SYSTEMS

FLIP's crew adjusted the starboard "blue" boom so it was aligned with and extended over the subsurface plume boom. An 8-lb lead sphere was lowered from the blue boom and used as a target to confirm the intersection of the acoustic beam with the sea surface (later, a standardized Bio-Sonics # 4 sphere was used for an *in situ* calibration check on the acoustic system). The lead sphere and taut line also served as a plumb, marking a point on the sea surface from which to align the video camera located on the aft boom. The microwave system, being rigidly attached to the video system, followed the same alignment. Figure 7 depicts the arrangement of the three booms (aft, blue, and plume) along with nominal acoustic and microwave footprints on the ocean surface.

7. SUMMARY OF DATA AND CONDITIONS

We had the misfortune of having the winds drop precipitously on day 3 (Year Day 19) (Fig. 2) of the experiment, just as various instruments were coming on line. During the period of relative calm between days 4 and 14 (Year Days 20–30), we

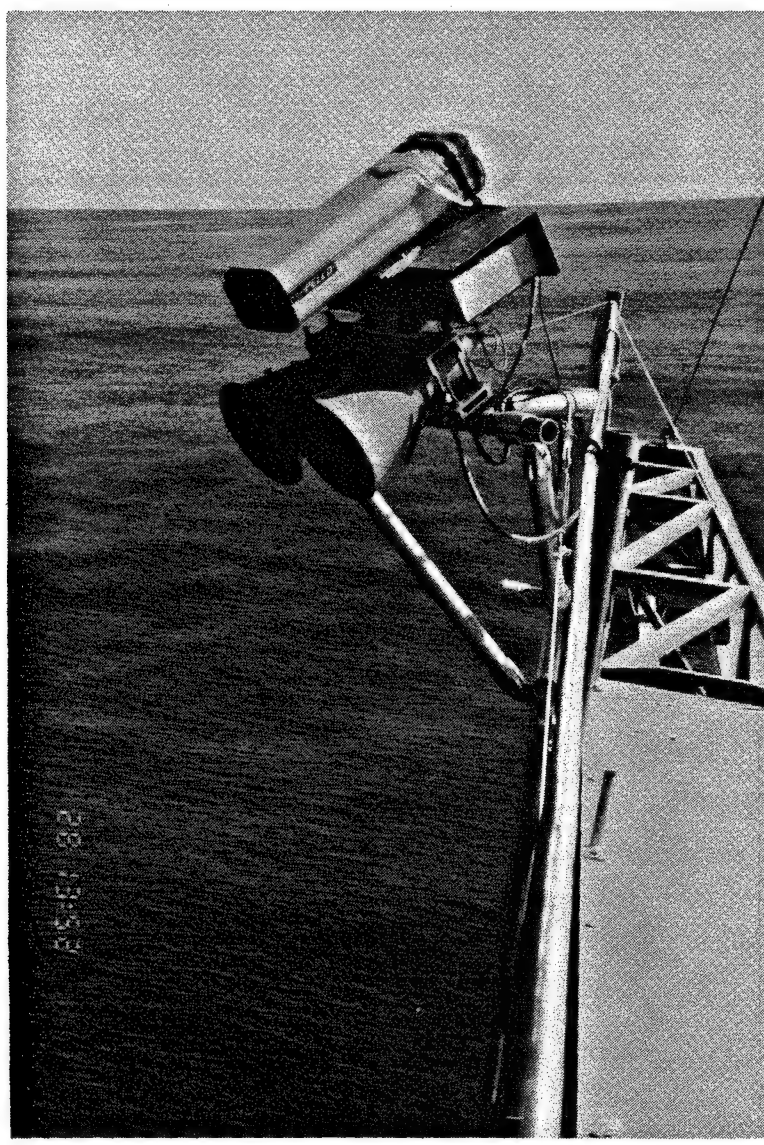

Figure 6. Photograph of the scatterometer and video camera mounted on *FLIP's* aft boom.

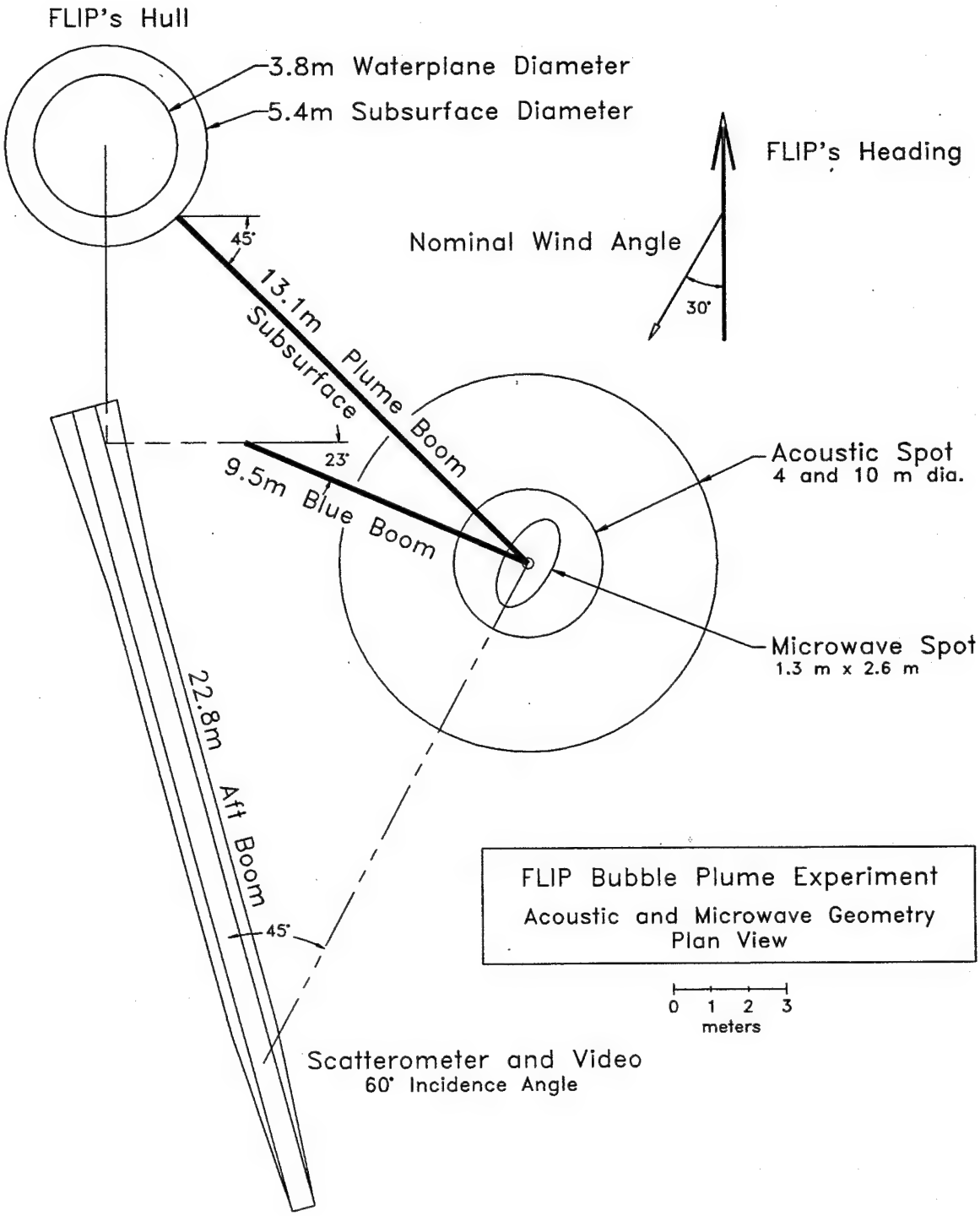

Figure 7. Alignment of aft and plume booms with *FLIP*'s hull, along with the acoustic and microwave footprints, or "spots," on the ocean surface.

collected the following kinds of data using the plume boom acoustic systems:

1. TARGET SPHERE—Backscattering from calibrated target spheres for *in situ* acoustic system calibration. Recent analysis of the data shows a measured target strength within 1 dB of sphere specifications, which confirms our system calibrations done at APL in December.

2. WATER COLUMN—Volume scattering measurements of the water column under calm water conditions, night vs. day. These data will serve as background for comparison with data taken during conditions characterized by wave breaking and a fully developed bubble field.

3. SIMULATED WAVE BREAKING—Acoustic measurements of simulated breaking waves. The waves were simulated by spilling a container of seawater over the active acoustic area. The container (either 5 or 15 gal) was lowered from the blue boom, and the water spilled by a trip wire from 1–3 m above the surface. Acoustic data were recorded at a 4-Hz ping rate starting a few seconds before the splash and continuing until steady state conditions returned. The splash was also recorded by the video camera.

Moderate winds returned for a brief period on day 12 (Year Day 28), disappeared, and then returned for good between day 15 and day 17 (Year Days 31–33). Our primary set of acoustic, microwave, and video (AMV) data was collected during this period. Our standard AMV run was made with a ping rate of 4 Hz for 10 continuous minutes (2400 pings). Appendix B summarizes all the acoustic data taken with the plume boom systems.

8. EXAMPLES OF ACOUSTIC SPACE-TIME IMAGES OF VOLUME SCATTERING BY BUBBLES AND DETECTION BY MICROWAVE AND VIDEO SYSTEMS

The output of our acoustic receiving system is a signal that has been heterodyned down to 5 kHz, regardless of transmit frequency, with a nominal bandwidth of 10 kHz. The conditioned 5-kHz signal is digitized at a 20-kHz rate, and the data are later digitally bandpass filtered between 1 and 9 kHz to remove distortions and noise that may have been introduced during the conditioning phase. Echo envelopes are computed from the Hilbert transform of each ping, or vector, of data. A sequence of pings forms a matrix from which we produce space-time images.

A measure of volume scattering is the scattering cross section per unit volume m_v in m^{-1} (formed by multiplying our backscattered measurements by 4π) and its

decibel equivalent M_v. We compute M_v as a function of range r derived from the time delay from the squared echo envelope using the sonar equation:

$$M_v(r) = RL(r) - SL + TL(r) - 10\log(V(r)) + 10\log 4\pi \ , \tag{1}$$

where

$RL(r)$ = backscattered pressure level, dB re μPa

SL = source level, dB re μPa at 1 m

TL = transmission loss, $40\log r + 2\alpha r$

$V(r)$ = sampling volume of a pulse.

Equation (1) provides a quick check on the data, but it does not include transmission loss due to extinction from the bubble layer. (That loss is perhaps 1–3 dB, causing an underestimate for bubbles located near the surface.)

Figure 8 shows 50 s of a space-time image of M_v taken at 30 kHz with our Mk 46 system. The data were obtained 31 January at 1630; the wind speed was approximately 10 m/s. Several features of the image are readily identified, starting with the time-varying free surface at approximately 30-m range from the sonar. The light blue (−50 dB level) streaks following the contour of the sea surface are enhanced volume backscatter due either to zooplankton, temperature anomalies, a trapped layer of bubbles, or a combination of these processes. The parcel of water responsible for the scattering clearly moves in phase with the surface wave motion; the amplitude is consistent with linear wave theory, which predicts an amplitude reduction of about 50% at 20-m depth.

Volume scattering from the bubble layer increases rapidly from −40 to −10 dB within the first 5–10 m of the surface. The scattering level and depth scale are consistent with recent measurements taken at 28 kHz under similar conditions.[1] The sea surface is markedly steep at about 9 s; during the next 30 s the bubble layer roughly doubles in thickness. Whether this increase is caused by advection of bubbles into the sonar beam or is the result of a breaking wave above the sonar remains to be determined.

The next image demonstrates how we can use the simultaneous acoustic, microwave, and video measurements to distinguish spatial from temporal effects in our data. Figure 9 shows 3 min of a space-time image of M_v taken at 240 kHz with our piston system shortly after the run in Fig. 8. The image shows bubble cloud growth

[1]S. Vagle and D. Farmer, "The measurement of bubble size distributions by acoustical backscatter," *J. Atmos. Oceanic Technol.*, in press

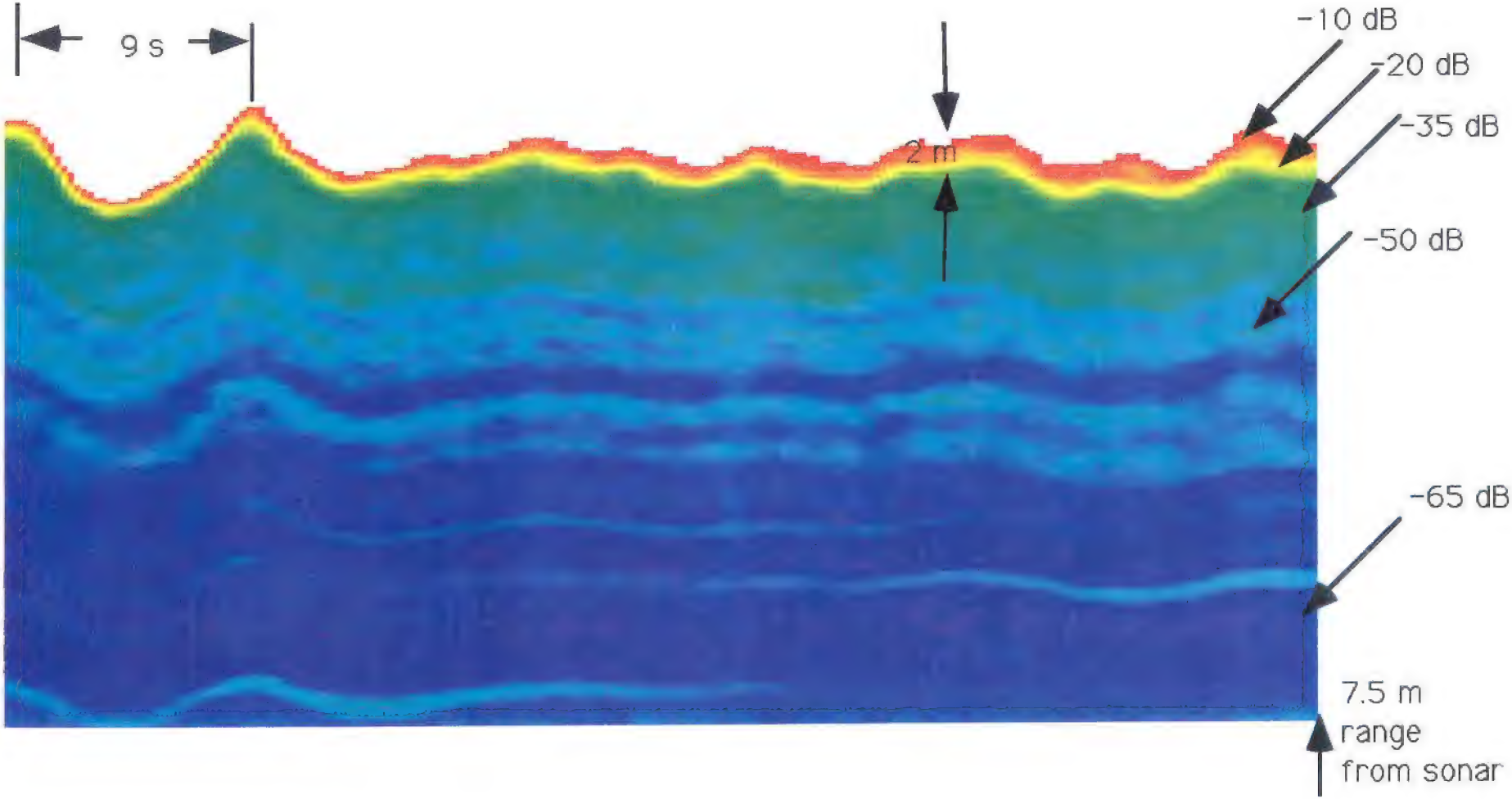

Figure 8. A space-time image of scattering strength per unit volume M_v taken at 30 kHz. The image represents 50 s of data (200 acoustic pings) from a 10-min run. The vertical axis represents the range from the sonar, beginning at 7.5 m and extending to an average height above the sonar of 28.5 m. The horizontal axis represents ping index or time. Colors corresponding to scattering levels between -10 and -65 dB are marked.

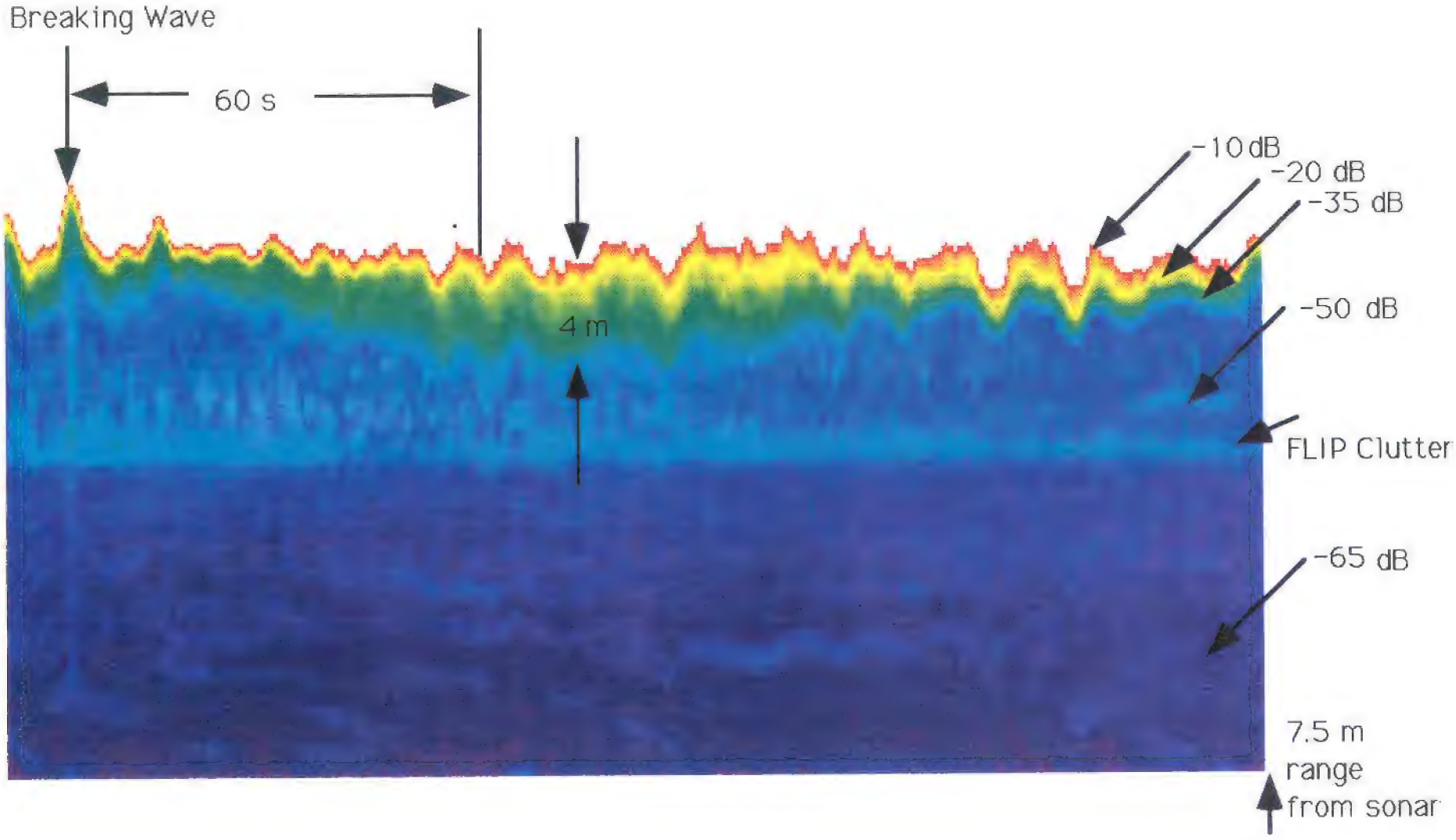

Figure 9. A space-time image of scattering strength per unit volume M_v taken at 240 kHz. The image represents 3 min of data (720 acoustic pings) from a 10-min run. The vertical axis represents the range from the sonar, beginning at 7.5 m and extending to an average height above the sonar of 28.5 m. The horizontal axis represents ping index, or time. Colors corresponding to scattering levels between −10 and −65 dB are marked. The arrow marking the breaking wave corresponds to second 218 of the 10-min run.

and decay within a period of about 1 min.[2] The rapid growth of this bubble layer is coincident with a large breaking wave (marked by the vertical arrow) occurring in the illumination area. The light blue vertical line aligned with the arrow may be evidence of a transient increase in ambient noise resulting from the breaking event. Figure 10 shows a time series of radar cross section, mean Doppler frequency, and Doppler bandwidth for the same 3-min period. A large jump in cross section (a so-called sea spike) and Doppler bandwidth is seen at second 218 (corresponding to the breaking wave in Fig. 9). The sea spike and increased Doppler bandwidth are evidence of a breaking wave, as verified by the video recordings. Figure 11 shows the foam and turbulence on the surface approximately 3 s after the breaking event; the video recording shows these persist on the surface for roughly 30 s.

9. DISCUSSION AND SUMMARY

We achieved our principal measurement objective of making simultaneous, *in situ* measurements of breaking waves and bubble plumes using acoustic, microwave, and video (AMV) systems trained on the same surface patch of the ocean.

We collected over 5 hours of AMV data; these were gathered at a rate of 4 Hz over a wind speed range of 4–11 m/s. A preliminary analysis of the vertical-incidence acoustic data shows that the background volume scattering strengths due to bubbles are consistent with those of data gathered under similar conditions.

Our acoustic system detected an increase in the bubble layer that may be associated with a whitecap simultaneously detected by our microwave and video systems.

The focus of our next report will be on identifying more simultaneously detected breaking waves and bubble clouds. We will begin the process of sorting out spatial from temporal effects in the structure of these bubble clouds by incorporating information on *FLIP*'s relative drift with respect to the bubble layer.

[2]The continuous line 20 m from the sonar is scatter from *FLIP*'s hull-mounted thruster. We don't see this scatter in Fig. 8 because a much lower source level was used. Scatter or "clutter" from *FLIP*'s hull is well documented in our calm-water data set taken a week earlier, and we expect to be able to subtract this clutter from our data.

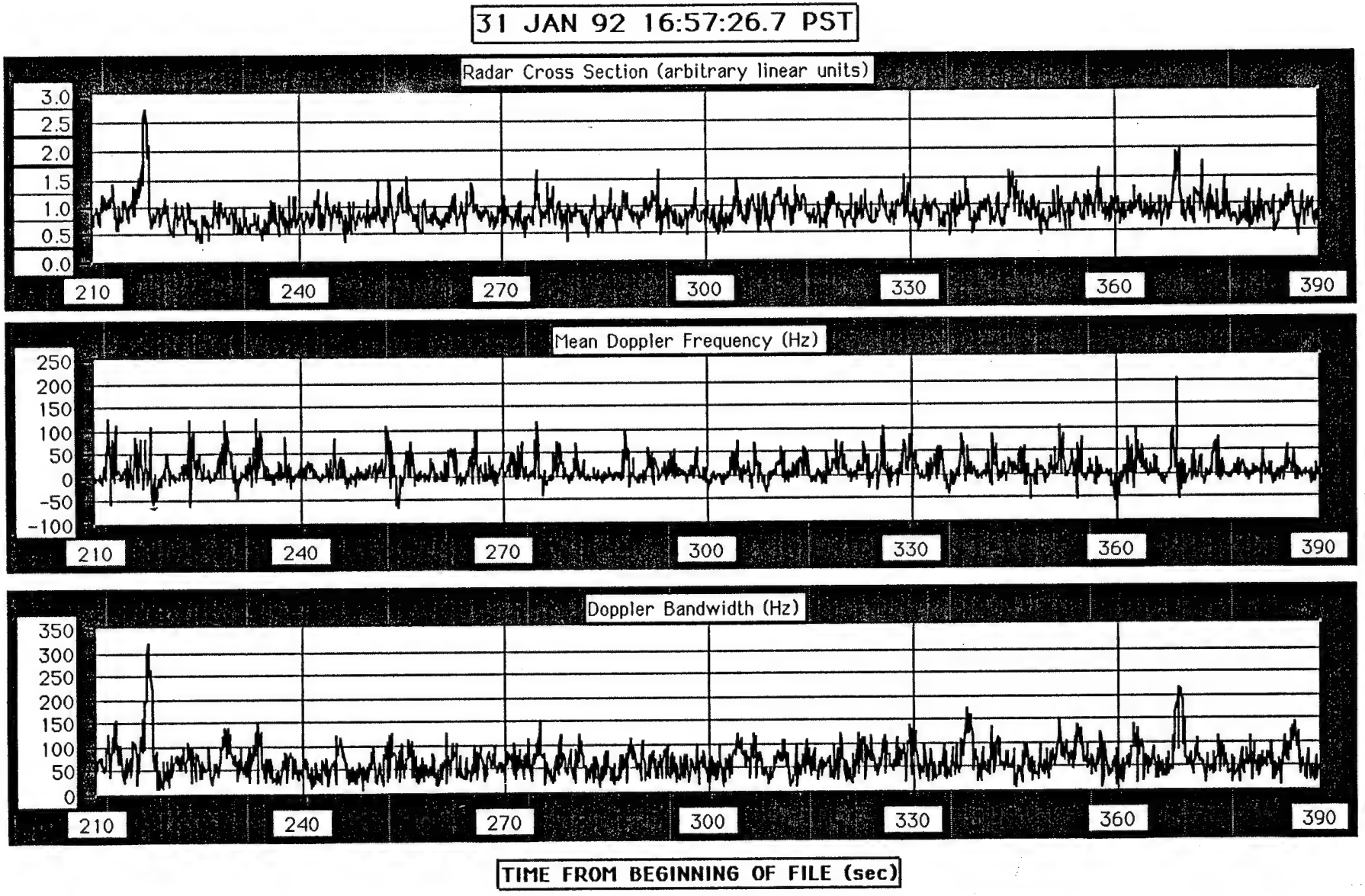

Figure 10. Time series of radar cross section, mean Doppler frequency, and Doppler bandwidth corresponding to the 3 min of acoustic data in Fig. 9. The large jumps in radar cross section and Doppler bandwidth at 218 s coincide with an increase in the bubble layer thicknes (Fig. 9) and the appearance of a whitecap in the illuminated area (Fig. 10).

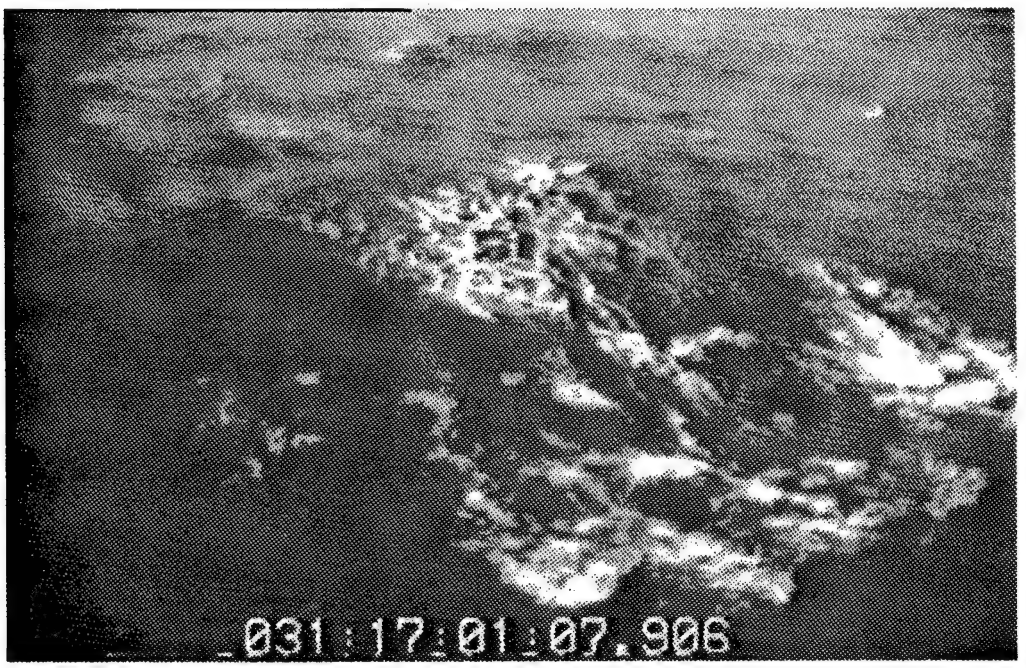

Figure 11. Video image showing foam and turbulence left behind by the breaking wave detected in the radar time series of Fig. 10 and coincident with the bubble plume shown in Fig. 9. The horizontal field of view is 16 m. The illuminated area is roughly in the center of the video image.

APPENDIX A: Overview of *FLIP-De Steiguer* TTCP Measurement Series

Objectives: Obtain coordinated measurements of acoustic surface scattering, the subsurface bubble field, and environmental sea surface conditions in order to examine the role of bubbles in near-surface acoustic scattering and propagation. These measurements will be used to develop and improve models used by designers of high frequency sonar systems for simulations that test and evaluate system concepts and prototypes.

Description: The experiment took place 400 n.mi. off the California coast (123° W, 34° N). A team from the University of Washington Applied Physics Laboratory (APL-UW) measured acoustic surface scattering (15–50 kHz) and environmental parameters from the research platform *FLIP*, and a team from the Institute of Ocean Sciences (IOS) measured the bubble field using its SEASAT instrument package deployed from USNS *De Steiguer*. (Arrangements were made by APL-UW with the Scripps Institution of Oceanography for use of R/P *FLIP* and the tow ship USNS *Navajo*, and with the U.S. Naval Oceanographic Office (NAVOCEANO) for USNS *De Steiguer*.) *De Steiguer* arrived at the experiment site on 12 January and began SEASAT deployments, which continued until departure on 24 January. *FLIP* arrived on 13 January under tow from USNS *Navajo*. Setup on *FLIP* required 3 days; measurements were taken between 16 January and 1 February. During the 9-day, two-vessel operation, *De Steiguer* kept station between 1 and 5 km from *FLIP*, following *FLIP*'s free drifting course. The operation was interrupted for 36 hours owing to an illness aboard *De Steiguer* that required a port call.

U.S. Role: APL-UW made acoustic forward scattering measurements using a source suspended from a 20-m spar buoy tethered to *FLIP* by a 1-km cable. Signals were received on horizontal and vertical 1.3-m line arrays, or on a Mk 46 torpedo head array, mounted on *FLIP*'s hull 66 m below the water line. Backscattering measurements were made with the Mk 46 system acting as the source/receiver. Ambient noise was recorded with omnidirectional hydrophones. Environmental measurements consisted of mean wind speed and direction (10-min averages) taken 10 and 25 m above the sea surface, surface wave-height spectra, air and sea temperatures, and CTD data. Additional CTD measurements were made aboard *De Steiguer* by a representative of NAVOCEANO.

Canadian Role: IOS deployed its SEASAT sonar drifter twice daily to measure features of the oceanic bubble field. The SEASAT collected multifrequency vertical incidence backscatter and horizontal-looking sidescan sonar data from a depth of 25 m. On three occasions, IOS deployed a portable acoustic source, supplied by APL-UW, from which acoustic data on forward scattering were recorded on *FLIP*.

During periods of calm weather, IOS also measured micro-bubble clouds formed by the wake of *De Steiguer*.

Results: The experiment successfully acquired acoustic, bubble field, and environmental data under conditions ranging from calm seas (Sea State 0) up to wind speeds of 20 kn (Sea State 4). IOS and APL-UW are in working-level contact, and the first priority is to isolate data most useful in quantifying the central role of oceanic bubbles in acoustic scattering and propagation.

APPENDIX B: Plume Boom Acoustic Data

file name	run type	date	time	wind	frequency	pulse
				(m/s)	(kHz)	length (ms)
vi-mk46.101	TARGET	18-Jan	1345	5.6	30	1
vi-mk46.102	TARGET	18-Jan	1352	5.4	30	1
vi-piston.112	TARGET	18-Jan	1423	6.7	240	0.5
vi-piston.113	TARGET	18-Jan	1500	6.4	240	0.5
vi-mk46.105	TARGET	20-Jan	1045	4.7	45	1
vi-piston.126	TARGET	20-Jan	1557	1.5	240	0.5
vi-mk46.107	TARGET	20-Jan	1720	2.4	45	1
vi-mk46.108	TARGET	20-Jan	1725	2.1	45	1
vi-piston.127	TARGET	20-Jan	1800	1.4	240	0.5
vi-mk46.113	WATER COLUMN	24-Jan	2006	3.8	40	1
vi-mk46.114	WATER COLUMN	25-Jan	1208	1.1	40	1
vi-mk46.115	WATER COLUMN	25-Jan	1320	1.3	40	1
vi-mk46.116	WATER COLUMN	25-Jan	1815	2.2	40	1
vi-mk46.117	WATER COLUMN	25-Jan	2330	1.2	40	1
vi-piston.185	WATER COLUMN	25-Jan	2400	1.1	240	0.5
vi-pison.190	WATER COLUMN	26-Jan	900	3	240	0.5
vi-mk46.118	WATER COLUMN	26-Jan	925	2.7	40	1
vi-mk46.119	WATER COLUMN	26-Jan	1753	2.6	40	1
vi-mk46.120	SIMULATED	26-Jan	1758	2.5	40	1
vi-mk46.121	WATER COLUMN	26-Jan	2400	2.8	40	1
vi-piston.193	WATER COLUMN	27-Jan	10	2	240	0.5
vi-mk46.123	WATER COLUMN	27-Jan	1325	3.5	40	1
vi-mk46.127	SIMULATED	27-Jan	1610	4.4	30	1
vi-mk46.128	SIMULATED	27-Jan	1630	4.4	30	1
vi-mk46.129	SIMULATED	27-Jan	1635	4.4	30	1
vi-mk46.130	SIMULATED	27-Jan	1657	4.4	30	1
vi-mk46.131	SIMULATED	27-Jan	1705	4.3	30	1
vi-mk46.132	SIMULATED	27-Jan	1716	4.3	30	1
vi-mk46.133	SIMULATED	27-Jan	1725	4.3	50	1
vi-mk46.134	SIMULATED	27-Jan	1738	4.3	50	1
vi-mk46.135	SIMULATED	27-Jan	1747	4.3	50	0.5
vi-mk46.136	WATER COLUMN	27-Jan	2015	3.1	40	1
vi-mk46.137	WATER COLUMN	27-Jan	2204	4.7	40	1
vi-piston.209	WATER COLUMN	28-Jan	830	0.6	240	0.5
vi-mk46.138	WATER COLUMN	28-Jan	900	0.6	40	1
vi-mk46.140	AMV	28-Jan	1650	4	40	0.5
vi-mk46.151	WATER COLUMN	28-Jan	2400	7.2	40	1
vi-mk46.152	SIMULATED	29-Jan	1420	5.2	30	0.5
vi-mk46.153	SIMULATED	29-Jan	1422	5.2	30	0.5
vi-mk46.155	SIMULATED	29-Jan	1501	6	30	0.5
vi-mk46.156	SIMULATED	29-Jan	1513	5.6	40	0.5
vi-mk46.157	SIMULATED	29-Jan	1523	5.5	30	0.5
vi-piston.237	TARGET	29-Jan	1550	5.9	240	0.5
vi-piston.238	TARGET	29-Jan	1544	5.9	240	0.5

vi-mk46.158	SIMULATED	29-Jan	1751	5.6	30	0.5
vi-mk46.159	SIMULATED	29-Jan	1755	5.6	30	0.5
vi-mk46.160	SIMULATED	29-Jan	1800	5.6	30	0.5
vi-mk46.161	WATER COLUMN	29-Jan	2234	2.7	30	0.5
vi-mk46.162	WATER COLUMN	29-Jan	2239	2.9	30	0.5
vi-mk46.163	WATER COLUMN	29-Jan	2247	2.9	40	0.5
vi-mk46.164	WATER COLUMN	29-Jan	2255	3.6	40	0.5
vi-piston.240	WATER COLUMN	29-Jan	2312	4	240	0.5
vi-piston.241	WATER COLUMN	29-Jan	2317	4	240	0.5
vi-piston.242	WATER COLUMN	29-Jan	2330	3.7	240	0.5
vi-mk46.166	SIMULATED	30-Jan	834	0.4	30	0.5
vi-mk46.168	SIMULATED	30-Jan	837	0.9	40	0.5
vi-mk46.169	SIMULATED	30-Jan	959	1.4	30	0.5
vi-mk46.170	SIMULATED	30-Jan	1000	1.5	30	0.5
vi-mk46.171	SIMULATED	30-Jan	1002	1.5	40	0.5
vi-mk46.172	SIMULATED	30-Jan	1018	1.5	30	0.5
vi-mk46.173	SIMULATED	30-Jan	1027	1.9	30	0.5
vi-mk46.174	SIMULATED	30-Jan	1038	1.8	30	0.5
vi-mk46.175	SIMULATED	30-Jan	1100	1.7	45	0.5
vi-mk46.208	SIMULATED	30-Jan	1630	3.6	30	0.5
vi-mk46.209	SIMULATED	30-Jan	1635	3.6	40	0.5
vi-mk46.210	SIMULATED	30-Jan	1638	3.6	30	0.5
vi-mk46.211	SIMULATED	30-Jan	1642	3.5	40	0.5
vi-piston.245	SIMULATED	30-Jan	1650	3.2	240	0.5
vi-mk46.216	SIMULATED	31-Jan	1015	6.8	40	0.5
vi-mk46.217	SIMULATED	31-Jan	1020	6.8	40	0.5
vi-mk46.218	SIMULATED	31-Jan	1030	6.8	30	0.5
vi-mk46.219	AMV	31-Jan	1041	7.2	30	0.5
vi-mk46.220	AMV	31-Jan	1052	7.2	40	0.5
vi-mk46.221	AMV	31-Jan	1111	8	30	0.5
vi-mk46.222	AMV	31-Jan	1123	7.1	40	0.5
vi-mk46.227	WATER COLUMN	31-Jan	1500	7.4	20-50	1
vi-piston.252	WATER COLUMN	31-Jan	1502	7.5	240	0.5
vi-mk46.228	WATER COLUMN	31-Jan	1516	7.7	30	0.5
vi-mk46.229	AMV	31-Jan	1630	10	30	0.5
vi-mk46.230	AMV	31-Jan	1642	9.2	30	1
vi-piston.258	AMV	31-Jan	1657	9	240	0.5
vi-mk46.231	AMV	31-Jan	1715	8.5	40	0.5
vi-mk46.232	AMV	31-Jan	1726	8.7	30	1
vi-mk46.237	WATER COLUMN	31-Jan	2400	6.3	20-50	0.5
vi-piston.263	WATER COLUMN	1-Feb	1	6.4	240	0.5
vi-mk46.240	WATER COLUMN	1-Feb	10	7	20-50	0.5
vi-mk46.241	AMV	1-Feb	1029	7.3	20-50	1
vi-mk46.242	AMV	1-Feb	1047	6.5	30	0.5
vi-mk46.243	AMV	1-Feb	1058	6.7	30	1
vi-mk46.244	AMV	1-Feb	1350	6.3	30	0.5

vi-mk46.245	AMV	1-Feb	1412	6.8	20-50	0.5
vi-mk46.246	AMV	1-Feb	1429	7.1	30	1
vi-mk46.247	AMV	1-Feb	1440	7.7	30	1
vi-mk46.248	AMV	1-Feb	1500	7.1	30	1
vi-piston.264	AMV	1-Feb	1525	7.1	240	1
vi-mk46.250	SIMULATED	1-Feb	1556	7.5	30	0.5
vi-mk46.251	SIMULATED	1-Feb	1604	7.3	30	0.5
vi-mk46.252	SIMULATED	1-Feb	1610	7.3	30	0.5
vi-mk46.253	SIMULATED	1-Feb	1614	7.3	30	1
vi-mk46.254	SIMULATED	1-Feb	1616	7.3	30	1
vi-mk46.255	SIMULATED	1-Feb	1620	7.3	30	1
vi-mk46.256	SIMULATED	1-Feb	1622	7.3	40	1
vi-mk46.257	SIMULATED	1-Feb	1626	7.3	40	1
vi-mk46.258	SIMULATED	1-Feb	1630	7.2	40	1
vi-mk46.259	SIMULATED	1-Feb	1633	7.2	30	1
vi-mk46.260	WATER COLUMN	1-Feb	1800	6.4	20-50	0.5
vi-mk46.266	WATER COLUMN	1-Feb	2212	5.7	20-50	0.5
vi-mk46.267	WATER COLUMN	1-Feb	2220	5.5	20-50	0.5
vi-mk46.268	WATER COLUMN	1-Feb	2230	5.4	30	0.5
vi-piston.265	WATER COLUMN	1-Feb	2255	5.6	240	0.5
vi-mk46.269	WATER COLUMN	2-Feb	816	4.7	20-50	0.5
vi-mk46.270	WATER COLUMN	2-Feb	820	5	20-50	0.5
vi-mk46.274	WATER COLUMN	2-Feb	830	5	30	0.5
vi-mk46.275	AMV	2-Feb	845	5	30	0.5
vi-mk46.276	AMV	2-Feb	858	5	30	1
vi-mk46.277	AMV	2-Feb	910	5	40	1
vi-piston.267	AMV	2-Feb	933	4	240	0.5
vi-piston.268	AMV	2-Feb	1520	5.5	20-50	0.5
vi-mk46.278	AMV	2-Feb	1530	5.5	30	0.5
vi-piston.269	AMV	2-Feb	1545	6.5	240	0.5
vi-mk46.279	AMV	2-Feb	1600	7	20	1
vi-mk46.281	AMV	2-Feb	1620	6.3	30	1
vi-mk46.283	TARGET	2-Feb	1645	6.3	30	1
vi-mk46.284	TARGET	2-Feb	1654	6.3	20	1
vi-mk46.285	TARGET	2-Feb	1655	6.3	40	1
vi-mk46.286	TARGET	2-Feb	1705	6.3	50	1
vi-piston.270	AMV	2-Feb	1710	7	240	0.5
vi-mk46.287	AMV	2-Feb	1725	6.5	30	1
vi-mk46.288	AMV	2-Feb	1740	6	30	0.5
vi-piston.271	AMV	2-Feb	1800	7.2	20-50	0.5

UNCLASSIFIED

SECURITY CLASSIFICATION OF THIS PAGE

REPORT DOCUMENTATION PAGE

Form Approved
OMB No. 0704-0188

1a. REPORT SECURITY CLASSIFICATION
Unclassified

1b. RESTRICTIVE MARKINGS

2a. SECURITY CLASSIFICATION AUTHORITY
NAVINST S5513.5A

2b. DECLASSIFICATION / DOWNGRADING SCHEDULE

3. DISTRIBUTION / AVAILABILITY OF REPORT
Approved for public release; distribution unlimited

4. PERFORMING ORGANIZATION REPORT NUMBER(S)
TM 2-92

5. MONITORING ORGANIZATION REPORT NUMBER(S)

6a. NAME OF PERFORMING ORGANIZATION
Applied Physics Laboratory
University of Washington

6b. OFFICE SYMBOL (*If applicable*)

7a. NAME OF MONITORING ORGANIZATION

6c. ADDRESS (*City, State, and ZIP Code*)
1013 N.E. 40th Street
Seattle, Washington 98105-6698

7b. ADDRESS (*City, State, and ZIP Code*)

8a. NAME OF FUNDING / SPONSORING ORGANIZATION
Office of Naval Research

8b. OFFICE SYMBOL (*If applicable*)
124

9. PROCUREMENT INSTRUMENT IDENTIFICATION NUMBER
N00039-91-C-0072

8c. ADDRESS (*City, State, and ZIP Code*)
800 N. Quincy Street
Arlington, Virginia 22217-5000

10. SOURCE OF FUNDING NUMBERS

PROGRAM ELEMENT NO.	PROJECT NO.	TASK NO.	WORK UNIT ACCESSION NO.
61153N			

11. TITLE (*Include Security Classification*)
Bubble Plumes and Breaking Waves: Measurements from R/P FLIP, January 1992

12. PERSONAL AUTHOR(S)
Peter H. Dahl and Andrew T. Jessup

13a. TYPE OF REPORT	13b. TIME COVERED	14. DATE OF REPORT (*Year, Month, Day*)	15. PAGE COUNT
technical	FROM _____ TO _____	May 1992	28

16. SUPPLEMENTARY NOTATION

17. COSATI CODES		
FIELD	GROUP	SUB-GROUP
20	01	
15	06	02

18. SUBJECT TERMS (*Continue on reverse if necessary and identify by block number*)
bubbles reverberation vertical incidence
breaking waves acoustic microwave low frequency

19 ABSTRACT (*Continue on reverse if necessary and identify by block number*)

This report is the first in a series of three covering APL-UW measurements of bubble plumes and breaking waves from R/P *FLIP* off the coast of California in January 1992. The overall objective of the experiment was to obtain realistic parameterizations of bubble plumes for use in models that predict low-frequency surface reveberation. The principal measurement objective was achieved: simultaneous, *in situ* measurements of bubble plumes and breaking waves using acoustic, microwave, and video systems trained on the same surface patch of the ocean. This report briefly summarizes the experiment, the range of environmental conditions encountered, the method of aligning the instruments, and the type and quantity of data gathered. Examples of acoustic data are given which clearly show bubble field growth; the appearance of one of these plumes was coincident with a wave-breaking event that was simultaneously detected with the microwave and video systems.

20 DISTRIBUTION / AVAILABILITY OF ABSTRACT
☒ UNCLASSIFIED/UNLIMITED ☐ SAME AS RPT. ☐ DTIC USERS

21. ABSTRACT SECURITY CLASSIFICATION
Unclassified

22a NAME OF RESPONSIBLE INDIVIDUAL
Dr. James Andrews

22b. TELEPHONE (*Include Area Code*)
703-696-5084

22c. OFFICE SYMBOL
ONR 124

DD Form 1473, JUN 86 *Previous editions are obsolete.*

S/N 0102-LF-014-6603

SECURITY CLASSIFICATION OF THIS PAGE

UNCLASSIFIED